POLITECNICO DI TORINO
Repository ISTITUZIONALE

The Oscillatory Behaviour of Cu-ZSM-5 Catalysts for N2O Decomposition: Investigation of Cu Species by Complementary Techniques

Original
The Oscillatory Behaviour of Cu-ZSM-5 Catalysts for N2O Decomposition: Investigation of Cu Species by Complementary Techniques / Rizzetto, A., Sartoretti, E., Khoma, K., Armandi, M., Piumetti, M., Bensaid, S., Pirone, R.. - In: CHEMPHYSCHEM. - ISSN 1439-7641. - ELETTRONICO. - (2024), pp. 1-13. [10.1002/cphc.202400339]

Availability:
This version is available at: 11583/2989555 since: 2024-07-30T09:00:05Z

Publisher:
Wiley

Published
DOI:10.1002/cphc.202400339

Terms of use:

This article is made available under terms and conditions as specified in the corresponding bibliographic description in the repository

Publisher copyright
Wiley postprint/Author's Accepted Manuscript

This is the peer reviewed version of the above quoted article, which has been published in final form at http://dx.doi.org/10.1002/cphc.202400339.This article may be used for non-commercial purposes in accordance with Wiley Terms and Conditions for Use of Self-Archived Versions.

(Article begins on next page)

18 November 2026

The oscillatory behaviour of Cu-ZSM-5 catalysts for N_2O decomposition: investigation of Cu species by complementary techniques

Andrea Rizzetto[a], Enrico Sartoretti[a], Khrystyna Khoma[a], Marco Armandi[a], Marco Piumetti*[a], Samir Bensaid[a], Raffaele Pirone[a]

[a] A. Rizzetto, Dr. E. Sartoretti, K. Khoma, Prof. M. Armandi, Prof. M. Piumetti, Prof. S. Bensaid, Prof. R. Pirone
Department of Applied Science and Technology
Politecnico di Torino
Corso Duca degli Abruzzi, 24, 10129 Turin (Italy)
E-mail: marco.piumetti@polito.it

Supporting information for this article is given via a link at the end of the document.

Abstract: Copper-exchanged ZSM-5 (Cu-ZSM-5) is a promising catalyst thanks to the Cu redox pair. A particular feature of this material consists in the presence of spontaneous isothermal oscillations which take place during N_2O decomposition reaction, depending on the operating conditions. In the present work, a set of five Cu-ZSM-5 catalysts are synthesised by three procedures and three different copper precursor concentrations: i) wet impregnation, ii) single ion exchange, and iii) double ion exchange. Catalytic tests reveal that the ion-exchanged samples exhibit a low catalytic activity and no oscillatory behaviour, except for the twice-exchanged sample which achieves an average N_2O conversion of 26 % at 400 °C. Conversely, the impregnated samples reach higher levels of N_2O conversion (66 % for Cu_5ZSM5_WI and 72 % for Cu_{10}ZSM5_WI) and demonstrate a similar oscillating pattern. Further investigations disclosed that the most active catalysts, characterised by the presence of oscillatory behaviour, have more abundant and easily reducible copper species (ICP, EDX and H_2-TPR) which interacts better with the zeolitic support (FT-IR). Catalytic tests under a long time on stream (TOS) suggest that either self-organised patterns or deterministic chaos can be achieved during the reaction, depending on the operating conditions, such as temperature and contact time.

Introduction

The study of Cu-containing zeolitic catalysts has been extensively documented for many years, highlighting their exceptional activity in the selective catalytic reduction (SCR) of NO_X emissions with ammonia [1]. Specifically, Cu–ZSM-5 systems have been widely investigated because of their high activity in the direct decomposition of NO. These materials are also effective in the conventional reduction with NH_3 (catalysed at very low temperatures) [2] and in the reduction of NOx with hydrocarbons and/or CO [3]. However, the decomposition of N_2O stands out as both the most intriguing and challenging reaction to investigate. This is not only because N_2O is a pollutant in its own right but also because it serves as a crucial intermediate in the decomposition of NO over this catalyst.

N_2O is considered a greenhouse gas and its influence on global warming is assessed by the so-called global warming potential (GWP). The GWP of nitrous oxide is 310 and 21 times larger than the values for carbon dioxide (CO_2) and methane (CH_4), respectively. Due to anthropological activities, the level of these three greenhouse gases has increased since 1850 at rates that have never been observed in the past 800,000 years [4,5]. Therefore, a reduction in their emissions is urgently required, and catalysis can play a significant role in this direction [6–10]. The catalytic decomposition of N_2O presents an efficient strategy for mitigating emissions of this gas, enabling the conversion into molecular nitrogen and oxygen as final products:

$$2\ N_2O \rightarrow 2\ N_2 + O_2 \qquad \text{Eq. (1)}$$

This reaction is particularly attractive since it does not require any reductant species and renders N_2O abatement possible at lower temperature ranges (300–500 °C) than the conventional thermal process.

Research into the Cu-ZSM-5 catalysed reaction of N_2O decomposition has revealed a fascinating characteristic of this material: it demonstrates oscillatory behaviour in the rate of N_2O decomposition. It has been observed that self-sustained isothermal oscillations in the outlet concentration of N_2O can occur when a flow of N_2O, diluted in an inert gas, passes over the Cu-ZSM-5 catalyst within a temperature range of 320 – 400 °C.

Lintz and Turek [11] were the pioneers in investigating the isothermal oscillation observed in N_2O decomposition over Cu-ZSM-5, uncovering random fluctuations in the concentrations of N_2O, NO, and O_2 during an experiment conducted at 450 °C.

On the other hand, Ciambelli et al. [12] observed the effects of both catalyst pre-treatment and reaction temperature on the oscillation behaviour and on the conversion yield. Experimental tests confirmed superior conversions in the case of reducing pre-treatments (most of the copper species in the Cu^+ form), compared to oxidising pre-treatments. Moreover, they found a connection between the oscillation frequency and reaction temperature [12]. Notably, the oscillating behaviour of mononuclear reactions is particularly rare and there are few examples reported in the literature; conversely, this peculiar attitude is typical of other bimolecular catalytic reactions, such as the oxidation of CO or NH_3 on metals, metal oxides and zeolites [13,14]. At the beginning of its study [12], the oscillatory behaviour was related to variations of the Cu oxidation states by N_2O molecule, which acts as both an oxidant and a reductant. Moreover, Ciambelli et al. [15] proposed the following reaction pathway involving Cu^+ centres:

$$2\,Cu^{+} + N_2O_{(g)} \rightarrow [Cu - O - Cu]^{2+} + N_{2\,(g)}$$ Eq. (2)

$$[Cu - O - Cu]^{2+} + N_2O_{(g)} \rightarrow 2\,Cu^{+} + O_{2\,(g)} + N_{2\,(g)}$$ Eq. (3)

$$[Cu - O - Cu]^{2+} \leftrightarrow 2\,Cu^{+} + O_{ads}$$ Eq. (4)

$$2\,O_{ads} \leftrightarrow O_{2\,(g)}$$ Eq. (5)

This mechanism foresees that a mono(μ-oxo)dicopper species $[Cu - O - Cu]^{2+}$ arises as a result of adsorption of a gaseous N_2O molecule on two vicinal Cu^{+} sites (Eq. (2)). In this first step N_2O acts as an oxidising species. Subsequently, the oxidised complex can react with a second N_2O molecule, which, in this case, acts as a reductant. The result of this second step is the regeneration of the two Cu^{+} sites and the release of molecular nitrogen and oxygen. Eq. 4 and 5 concern the probability of spontaneous desorption of extra-lattice oxygen (ELO) from $[Cu – O – Cu]^{2+}$ species as dioxygen molecule. The cause of these fluctuations has been assumed to be the different speed between these reactions: the formation of the mono(μ-oxo)dicopper complex is the fastest one, due to the presence of active Cu^{+} sites, while both the fourth and the fifth stages are rate-limiting.

The preparation techniques employed on Cu-ZSM-5 catalysts could affect the presence of oscillations [16]. Notably, the ion-exchange synthesis is able to promote the generation of vicinal Cu^{+} sites, capable to form $[Cu - O - Cu]^{2+}$ species, especially with copper cations in excess with respect to zeolite sites ("over-exchange synthesis") [15,17,18]. Changing the synthesis procedure may give rise to different oxidation states and dispersion of copper. For instance, Shpiro et al. [19] observed that Cu-ZSM-5 prepared through impregnation method led to the formation of large aggregates at the zeolite external surface.

In our previous study [13] we found superior N_2O decomposition activity and pronounced oscillations for Cu-ZSM-5 materials prepared by impregnation procedure. These findings were related to the nature of copper "excess" and the occurrence of oligomeric Cu_xO_y species with extra-lattice oxygen (e.g., chains or clusters).

The aim of the present study is to delve into the isothermal oscillating behaviour observed in the decomposition of N_2O. To achieve this, a variety of Cu-ZSM-5 catalysts was synthesized using either wet impregnation or ion-exchange procedures. The physico-chemical and surface properties of the prepared materials were examined using complementary techniques, such as variable temperature FT-IR spectroscopy, H_2-TPR (Temperature Programmed Reduction) analysis, XRD, N_2 physisorption at -196 °C, ICP-MS, HRTEM, and EDX spectroscopy. Catalytic tests were conducted under varying conditions to explore their impact on the catalysts' performance.

Materials and experimental methods

Catalysts preparation

NH_4-ZSM-5 with Si/Al ratio of 25 was used as parent zeolite and was calcined at 550 °C in an air atmosphere for 5 h to obtain the protonated form, in order to make the support more stable to subsequent heat treatments. Three types of synthesis were performed. Two different i) ion-exchanged catalysts (IE) were prepared with a 10 mM or 5 mM solution of copper (II) acetate monohydrate ($Cu(CH_3COO)_2{\bullet}H_2O$, Sigma Aldrich, 99 %), respectively. Solutions with the same concentrations were adopted to synthesize two ii) wet-impregnated (WI) samples. A fifth catalyst was made through iii) two subsequent ion-exchanges with a 25 mM copper acetate solution (IE2).

Ion-exchanged samples (i) were synthetized as follow: the copper precursor was mixed with 100 mL of distilled water and 1 g of H-ZSM-5. Subsequently, the mixture was kept under vigorous stirring at room temperature (RT) for 2h. Finally, the ion-exchanged zeolite was recovered by centrifugation, washed three times with distilled water, and dried overnight at 60 °C.

Similarly to the ion-exchanged samples, the impregnated zeolites (ii) were obtained by mixing $Cu(CH_3COO)_2{\bullet}H_2O$ with 100 mL of distilled water and 1 g of H-ZSM-5. The solution was kept under vigorous stirring at 100 °C, until complete evaporation of water. Afterwards, the slurries were dried overnight at 60 °C.

The ion-exchange procedure was repeated twice in the case of double ion-exchanged catalyst (iii). All the samples (i, ii, iii) were finally calcined under a N_2 flow (200 mL min^{-1}) at 550 °C for 2 h and subsequently under a flow of 1%-vol O_2 in N_2 (200 mL min^{-1}) at 550 °C for 2 h. The following nomenclature was assigned to the catalysts prepared in this work: Cu_xZSM5_y where "x" refers to the molar concentration of copper acetate precursor (mmol L^{-1}) and "y" indicates the synthesis method (WI, wet impregnation, IE, ion-exchange, and IE2, double ion-exchange).

Physico-chemical characterizations

The copper loading of each catalyst was confirmed with the aid of a Thermo Scientific iCAP RQ ICP-MS device. First, powder catalysts were dissolved in a mixture of hydrofluoric acid, phosphoric acid, and sulfuric acid (2 mL: 4 mL: 4mL) by the mean of microwave-assisted digestion at

220 °C for 15 min (heating rate 10 °C min^{-1}). Afterwards, the digestates were diluted to obtain the suitable metal concentration for the elemental analysis.

The crystalline nature of materials and the presence of CuO clusters were elucidated by X-Ray Diffraction (XRD) measurements performed by the means of X Pert PANalytical diffractometer (Cu Kα radiation) equipped with a PiX accelerator detector. Powder data were collected on a flat zero background sample holder. Bragg-Brentano geometry was used to acquire the XRD pattern in the range of 5–70° 2θ angles using the ¼-¼ pair of optical slits (voltage 40 kV; current 40 mA). HighScore Plus® software was employed to identify the phases characterizing the samples.

Porosimetric measurements were performed through nitrogen physisorption at 77 K, using a Micromeritics ASAP TRISTAR 3020 instrument. Prior to the analysis, all the catalysts underwent a pre-treatment consisting in heating in nitrogen flow at 200 °C for 2 hours in a specifically dedicated system (Micromeritics FlowPrep 060), to eliminate possible adsorbed components on the material. The specific surface area was calculated with Brunauer-Emmett-Teller (S_{BET}) method in the relative pressure range from 0.05 to 0.15, while the pore volume was assessed at the relative pressure of 0.9.

X-ray photoelectron spectroscopy (XPS) investigation of the catalyst powder was performed with PHI 5000 Versa Probe instrument, equipped with a monochromatic Al K-alpha X-ray source (1486.6 eV) and the obtained spectra were processed with Casa XPS software (Version 2.3.18). High-resolution (HR) Cu 2p core-level spectra were acquired with long acquisition times, due to the scarce abundance of this element in the catalysts. Spectra were charge corrected so that the main line for the carbon 1 s spectrum (adventitious carbon) was set to 284.8 eV.

The catalysts' reducibility was evaluated by H_2-TPR (Temperature Programmed Reduction) analysis on a Thermo Scientific TPDRO 1100 equipped with a thermal conductivity detector (TCD). 50 mg of sample were pre-treated in a He stream with a heating ramp (550 °C, 10 °C min^{-1}). After 60 min at 550 °C, the reactor was cooled down in a stream of He. The sample was then heated from 50 up to 550 °C with a 10 °C min^{-1} ramp while flowing 20 mL min^{-1} of 5% H_2 in He.

Fourier transform infrared spectroscopy (FTIR) was carried out by using a Bruker Invenio S spectrometer equipped with an MCT detector. Spectra of Cu-ZSM-5 catalysts were recorded in transmittance mode in the region ranging from 4000 to 800 cm^{-1} at a spectral resolution of 2 cm^{-1}. The samples were pressed at 2 tons to obtain a thin tablet and embedded within a quartz IR cell equipped with KBr optical windows. Although tablets with comparable area and weight were prepared, all the spectra were normalized with respect to the integrated absorption of framework overtone bands (2090 – 1550 cm^{-1}). Firstly, a room-temperature spectrum was acquired; thereafter, each sample was degassed at 10^{-4} mbar and treated at 500 °C (heating ramp 5 °C min^{-1}) for 1 h by connecting the IR cell to a high vacuum line.

Variable-temperature infrared spectroscopy (VT-IR) was performed in a Bruker Tensor 27 using a commercial IR cell (AABSPEC), equipped with a capacitance pressure sensor (CTR100, Oerlikon-Leybold) and an electronically-controlled heating device. A K-thermocouple was placed in contact with the sample wafer to monitor the actual temperature inside the cell. For each VT-IR measurement, the sample was activated (outgassed) in the same vacuum line for 1 h at 500 °C. Thereafter, the cell was cooled to room temperature and filled with ca. 30 mbar of N_2O, after which the cell was closed, and IR spectra were collected at several scheduled temperature values within the range 200-400 °C (spectral resolution of 2 cm^{-1}). The schematic procedure adopted for the variable temperature experiments is depicted in **Fig. S1** in the S*upporting Information file*.

EDX analysis was performed in a Zeiss Merlin electron microscope with a Gemini-II column and an Oxford x-act X-ray detector for energy dispersive X-ray spectroscopy (EDX). The elemental copper distribution was investigated by acquiring EDX spectra over different points for each sample.

Furthermore, images were acquired by the mean of high-resolution transmission electron microscopy (HRTEM) using a Thermo Scientific Talos F200X microscope operated at 200 kV, equipped with a detector for energy dispersive X-ray spectroscopy (EDX). The sample powder was suspended in high-purity 2-propanol and then dripped on the holey carbon film of a gold support grid. EDX maps in scanning-transmission mode (STEM) were collected to investigate the elemental distribution.

The N_2O catalytic decomposition experiments were performed with an experimental set-up consisting of a quartz U-shaped reactor, a furnace, and gas analysers. The reactor, located in a CARBOLITE GERO® Tube Furnace, was connected to the inlet gas through a stainless-steel tube with an outer diameter (O.D.) of 1/4". The gas implant was equipped with an EMERSON X-STREAM XE gas analyser, provided with a nondispersive infrared detector for N_2O, NO, NO_2 and a paramagnetic sensor for O_2. A K-type thermocouple monitored the reactor temperature during the process. A set of Brooks® mass flow controllers regulated the gas inlet flow rate. Catalytic tests were carried out using a mixture of 1000 ppm of N_2O in He (200 mL min^{-1}) at three different temperatures, namely 350, 375 and 400 °C. Before the tests, 100 mg of catalyst were pelletized, crushed, and sieved (500-250 μm), and loaded into the U-shaped reactor. Each catalyst underwent a pre-treatment consisting of a thermal activation at 550 °C for 2 h in He (200 mL min^{-1}), and then the system was cooled down to reach the experimental temperature.

Results and Discussion

Investigation on the catalytic activity

The evolution of N_2O outlet concentration during the isothermal conversion at 400 °C over the five Cu-catalysts is depicted in **Fig. 1a**. All catalysts show a rather variable capacity in the decomposition of N_2O, related to the amount of copper contained in the samples, which is affected by the synthetic method (see *Characterization of structural and textural properties*). Cu_5ZSM5_IE and Cu_{10}ZSM5_IE have almost the same low Cu content (around 1 wt.%) and were able to convert only a low and similar percentage of the fed N_2O, namely 2 and 3 %, respectively, with a linear conversion profile. Conversely, Cu_5ZSM5_WI, Cu_{10}ZSM5_WI, and Cu_{25}ZSM5_IE2 contain higher Cu loadings (ca. 3.2, 5.9, 1.8 wt.%, correspondingly) and reached a superior percentage of N_2O abatement, i.e., 66, 72 and 26 % respectively. It is particularly noteworthy that Cu_5ZSM5_WI and Cu_{10}ZSM5_WI are characterised by a close value of conversion, although the latter sample possesses an almost double quantity of Cu. Moreover,

the average conversion capacity of Cu_{25}ZSM5_IE2 is almost 1/3 of that of Cu_5ZSM5_WI, even though the Cu content of the former sample is around ½ with respect to that of the latter material. For all three catalysts, the outlet N_2O concentration did not reach a stable and constant value during the time on stream (TOS), but exhibited an oscillating pattern, in agreement with previous works [16,20,21]. Considering the intensity of oscillations, Cu_{10}ZSM5_WI demonstrated more stable and constant negative peaks than the other catalysts, whose oscillations were less regular and increased in intensity during the time on stream. A magnification of the fluctuation in the range from 80 to 140 min for the three oscillating catalysts is depicted in **Fig. 1b**. The oscillation frequency seems to be not correlated with the copper content. However, it is noteworthy to observe that there is a certain similarity between the periods of the conversion curves of the two impregnated samples; conversely, the double ion-exchanged sample exhibits a slightly different oscillation profile, which can be traced back to the synthesis technique used. Another significant singularity is related to a sort of "ignition time" before the beginning of the oscillations. The impregnated samples took ca. 30 minutes before showing oscillations, while the ignition time of the exchanged one lasted ca. 15 minutes. Cu_5ZSM5_IE and Cu_{10}ZSM5_IE also showed a sort of ignition time, observable from the small hump at the beginning of their average conversion profile.

In order to study the behaviour of these unsual catalysts in more detail, the profiles of the output concentration of N_2O, NO, NO_2 and O_2 gases were recorded during the catalytic tests and, for the sake of simplicity, the trends for the Cu_5ZSM5_WI and Cu_{10}ZSM5_WI catalysts are depicted in **Fig. 2**. According to the N_2O decomposition reaction (Eq. (1)), one of the main products is oxygen, whose outlet concentration follows the oscillatory movement of the N_2O concentration exactly in antiphase with respect to the protoxide period (**Fig. 2a**). The stoichiometric ratio between the two gases is, on average, agreeable, even if the shape of the two signals appears non-specular and somewhat different. Moreover, the oscillation of N_2O is accompanied by the oscillating by-production of NO and NO_2, as well, whose presence is unforeseen by the decomposition reaction of the protoxide (**Fig. 2b**). The presence of NO_x species in the decomposition of N_2O has already been observed in the literature [16,20], and can be linked to the formation of nitrates on the active sites of the catalyst [22], as pointed out in the present study through VT-IR experiments (see *Study of the catalyst surface properties*). Considering the decomposition reaction (Eq. 1), nitrogen monoxide can be formed as an intermediate in the reduction reaction of N_2O, as illustrated in Ochs and Turek's mechanism (step c - see *Study of the catalyst surface properties*) [20]. Thus, in the presence of oxygen produced by the main reaction, some of the NO can be further oxidised to NO_2 according to the reaction $2\ NO + O_2 \rightleftharpoons 2\ NO_2$ [23]. The NO_X profiles appear in the form of simultaneous peaks rather than oscillations, and the ratio between the two gases is probably fixed at its thermodynamic limit value because Cu-ZSM-5 strongly activates the conversion of NO to NO_2 [24].

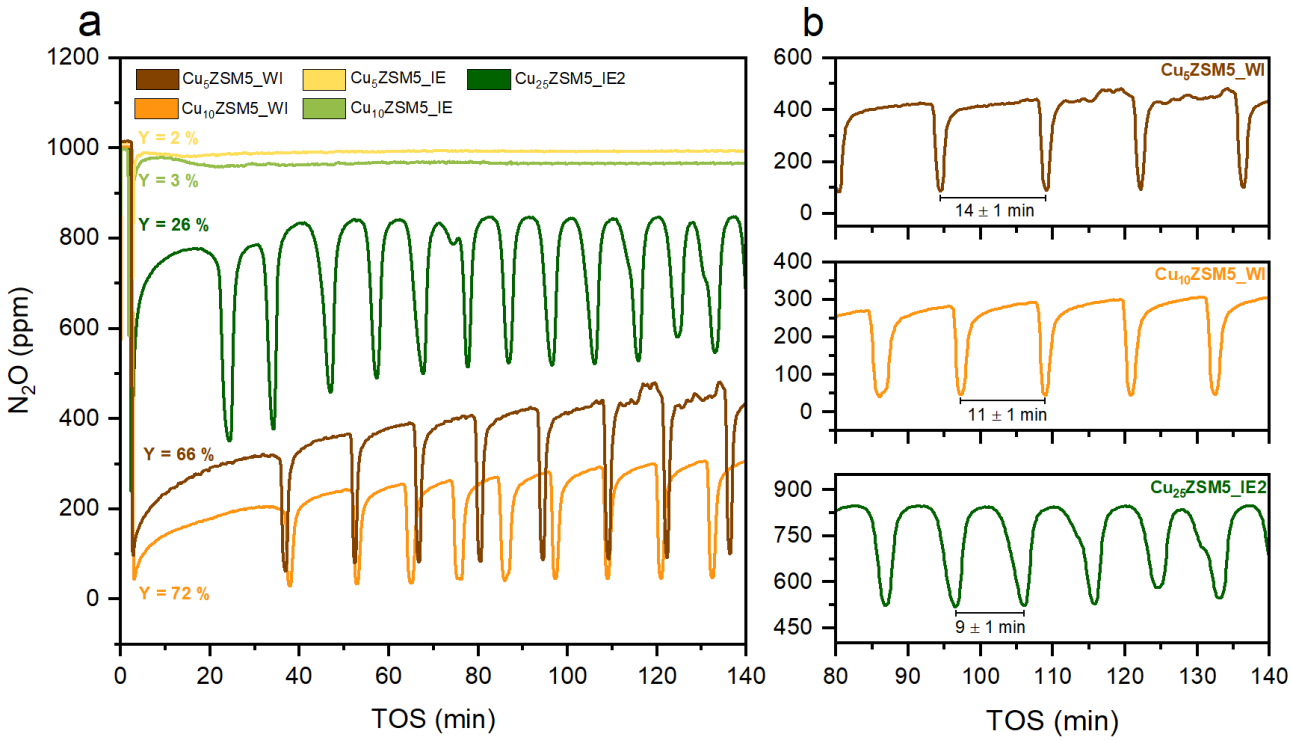


Figure 1 (a) Evolution of N_2O outlet concentration during the catalytic activity testing under isothermal experiments at 400 °C and **(b)** magnification of the oscillatory behaviour of Cu_5ZSM5_WI, Cu_{10}ZSM5_WI, and Cu_{25}ZSM5_IE2.

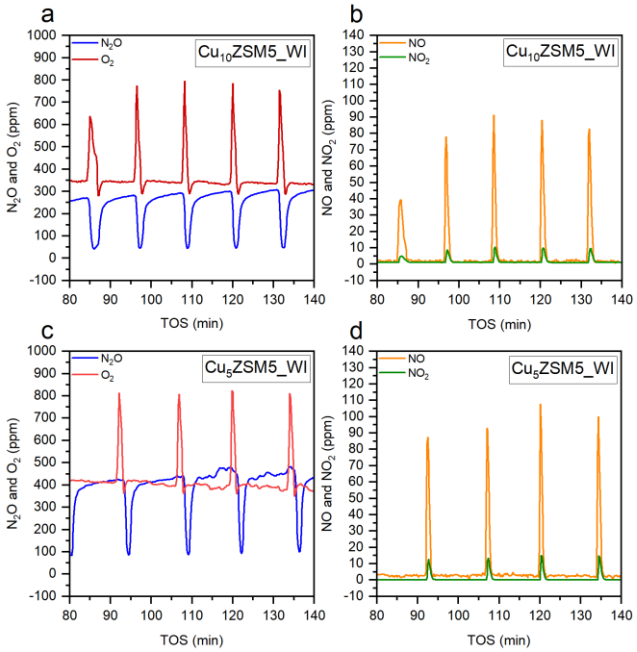


Figure 2: Concentration of N_2O, O_2, NO, and NO_2 at the reactor outlet during the catalytic activity testing under isothermal condition at 400 °C of Cu_{10}ZSM5_WI (**a, b**) and Cu_5ZSM5_WI (**c, d**).

The behaviour of NO and NO_2 is also characterised by maxima in antiphase with respect to the decomposition profile of N_2O, with their peaks at the minimum of the protoxide curves. This behaviour was a general trend over all N_2O decomposition tests in which fluctuations were observed. The aforementioned considerations asserted for the Cu_{10}ZSM5_WI sample can also be applied to the catalyst prepared with the lower copper amount, Cu_5ZSM5_WI (**Fig. 2c** and **2d**). Obviously, the magnitude of the gases produced by the conversion of N_2O reflects the abatement yield for both O_2 and the by-products NO and NO_2. Ochs and Turek [20] proposed in their work a potential justification for the development of isothermal oscillations. They assumed a sort of deactivation of the monovalent copper sites due to atomic oxygen deposition from N_2O interaction. The occupation of the copper sites proceeds with new N_2O molecules interacting with the catalyst, although some of this adsorbed oxygen may create intermediate species, NO_3, in a slow parallel reaction. When a critical oxygen coverage is reached, NO_3 decomposes into O_2 and NO. After NO release from the catalyst, the oscillatory cycle begins again with a new oxygen uptake.

The catalysts capable of oscillating, i.e., Cu_5ZSM5_WI, Cu_{10}ZSM5_WI and Cu_{25}ZSM5_IE2, were subjected to further tests at lower temperatures (375 and 350 °C) to better investigate the catalytic behaviour upon temperature variation. The outcomes shown in **Fig. 3** reveal that all three catalysts show periodic oscillations even at lower temperatures. However, the temperature change induces a modification in the oscillation pattern, with an associated decrease in the oscillation frequency for all three catalysts. The average conversion is also obviously affected by temperature variation, reaching a minimum of 12 % for Cu_5ZSM5_WI and Cu_{10}ZSM5_WI at 350 °C, while for Cu_{25}ZSM5_IE2 the yield drops to 4 % at the same temperature. Cu_5ZSM5_WI and Cu_{25}ZSM5_IE2 show fairly repetitive patterns at 375 °C, while the profile of the Cu_{10}ZSM5_WI catalyst is more irregular. Finally, at a lower temperature, the periods expand considerably and possess a particular irregularity.

Considering the periodicity of the oscillations, one can assume that, under specific operating conditions, the decomposition of N_2O over Cu-ZSM-5 catalysts can give rise to self-organized patterns as illustrated in **Fig. 4a**. In the present case, uniform oscillations with a well-defined periodicity can be achieved at 400 °C after an induction period. The existence of oscillating reactions in scientific literature is well-known [25], and one of the universal mechanisms of such pattern formation is the Turing instability [26]. In such scenarios, we observe Oscillatory Turing Patterns (OTPs), which represent a complex phenomenon where chemical reactions and diffusion processes interact to produce spatially periodic structures or temporal oscillations in a chemical system. These patterns are named after Alan Turing, who first theorized such mechanisms in 1952, suggesting that non-uniform distributions of chemical species could arise from homogeneous initial conditions through a process known as reaction-diffusion. An OTP signifies a state where the system exhibits both spatial and temporal periodicity due to the intrinsic properties of the reaction coupled with the diffusion of reactants and products. This leads to the appearance of oscillations in concentration over time, creating a dynamic pattern that is both predictable and self-sustaining under stable conditions.

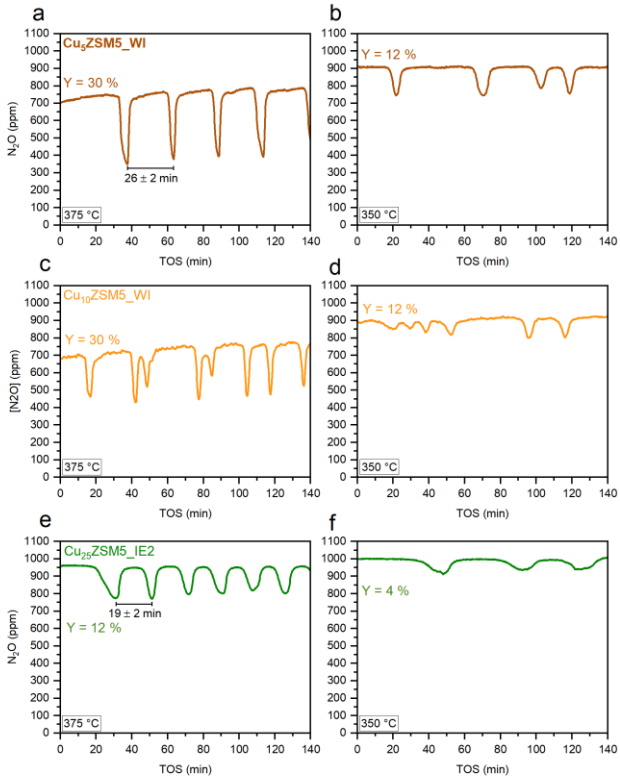


Figure 3: Evolution of N_2O outlet concentration during the catalytic activity testing under isothermal experiments at 375 °C **(a)**, **(c)**, **(e)** and at 350 °C **(b)**, **(d)**, **(f)** of Cu_5ZSM5_WI, Cu_{10}ZSM5_WI, and Cu_{25}ZSM5_IE2

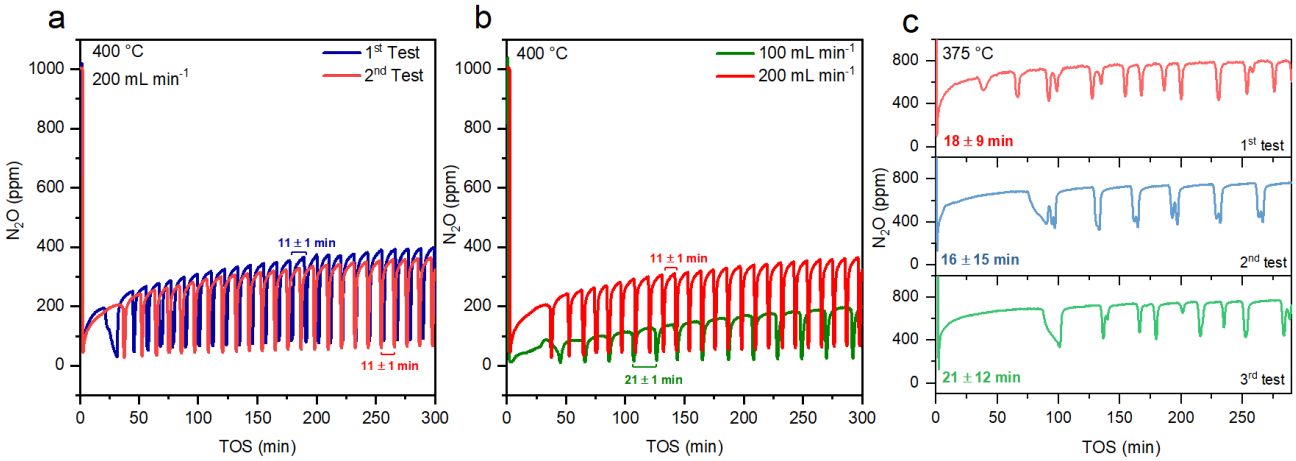


Figure 4: Evolution of N_2O outlet concentration of Cu_{10}ZSM5_WI during **(a)** catalytic tests performed at 400 °C (test and re-test) with a flow rate of 200 mL min^{-1} and **(b)** with different flow rates, namely 100 and 200 mL min^{-1}. **(c)** N_2O outlet concentration obtained with three tests at 375 °C (test, re-test 1 and re-test 2) with a flow rate of 200 mL min^{-1}. The average period of N_2O oscillations and the respective standard deviation are also reported for each curve in the figure.

Experiments performed with a different flow rate (**Fig. 4b**) confirmed that this reaction is particularly affected by the contact time between N_2O and Cu sites. As mentioned before, the oscillation could be caused by a deposition-inhibition phenomenon by N_2O decomposition. It may therefore be correct to infer that lowering the spatial velocity of the polluted gas slows down the phenomena of species coverage and accumulation [20]. As a result, the frequency of oscillations also decreases. Conversely to the experiments at 400 °C, under diverse operational conditions, the same catalyst can exhibit deterministic chaos at a different temperature, as depicted in **Fig. 4c**. This chaotic behaviour is characterized by an unpredictable and complex system response that, albeit deterministic at a fundamental level, appears random and lacks a clear pattern over time. Such deterministic chaos in catalytic reactions indicates a high dependence on the operating conditions, in contrast with the orderly and regular nature of Turing Patterns.

Characterization of structural and textural properties

An accurate elemental analysis of the as-prepared catalysts was performed by employing two techniques, i.e., ICP-MS and EDX, with the aim of evaluating the actual Cu content. The outcomes of these investigations are shown in **Table 1**. As expected, the copper loading obtained for the impregnated samples reflected more closely the quantity of metal present in the starting solution. Actually, the synthesis of these samples involves the total evaporation of water from the acetate solution in the presence of the support, ensuring efficient metal deposition. On the other hand, the limited number of acid sites in the zeolitic framework allows only partial proton exchange with metal ions. This limitation can be seen in the results of elemental analysis for exchanged zeolites: Cu_5ZSM5_IE and Cu_{10}ZSM5_IE samples possess almost the same amount of copper. Hence, a more concentrated solution of the metal cation only slightly promoted the exchange strength. Instead, exchange was greatly increased by performing two consecutive exchanges with fresh solutions of copper acetate [27], nearly doubling the content of Cu with respect to that of samples obtained by single ion exchange.

Theoretically, a single divalent Cu^{2+} cation is only able to neutralise two negative charges in the zeolite if they are sufficiently close to each other. This condition occurs most easily in the case of zeolites with a low Si/Al ratio. Therefore, the copper content is usually constrained below the 100 % exchange level (Molar Cu/Al < 0.5) in the ion-exchanged samples [28,29].

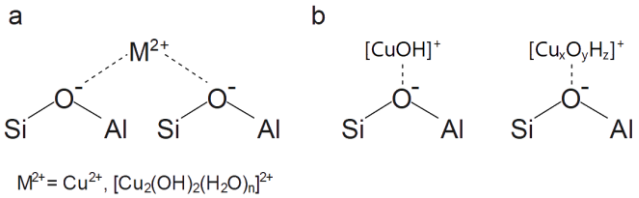
Table 1. Summary of physico-chemical features of the prepared catalysts.

Sample	Cu wt. % (ICP-MS) [(a)]	Cu wt. % (EDX) [(b)]	Cu/Al [(b)]	S_{BET} ($m^2\ g^{-1}$) [(c)]	V_{pore} ($cm^3\ g^{-1}$) [(d)]	%EX [(e)]
Cu_5ZSM5_WI	3.2	3.91	1.2	326	0.18	83
Cu_{10}ZSM5_WI	5.93	5.93	1.8	329	0.18	83
Cu_5ZSM5_IE	0.96	1.21	0.3	380	0.21	33
Cu_{10}ZSM5_IE	1.08	1.42	0.4	369	0.20	58
Cu_{25}ZSM5_IE2	1.78	2.35	0.7	359	0.20	54

(a) The quoted value is an average between two parallel analyses conducted on the same sample.
(b) The quoted value is an average between four areas of the sample analysed by EDX spectroscopy.
(c) Total specific surface area as measured by N_2 physisorption.
(d) Total pore volume as measured by N_2 physisorption.
(e) Percentage of exchange calculated by intensity ratio between the integrated IR absorbance of the 3610 cm^{-1} band in the pristine H-ZSM-5 and of the same band in the samples.

However, the procedure used to exchange a zeolite with a metal must be taken into account. One of the traditional methods for obtaining Cu zeolites is wet ion exchange. The copper precursor is prepared in an aqueous solution in which hydrolysis of the copper salts occurs, and part of Cu^{2+} is exchanged as $(Cu^{2+}\text{-}OH)^+$, a species that can be produced by the cleavage of an H_2O molecule in the Cu^{2+} hydration sphere (pH-dependent step) [30]. This condition is thermodynamically favoured since it is energetically more convenient to balance the lattice charge with monovalent cations than with a divalent cation, especially in silica-rich zeolites where the negatively charged Al-T sites are widely separated from each other. Moreover, the Cu hydrolysis accompanies zeolite ion-exchange and results in the formation of dimers and copper polyhydroxide complexes $(Cu_xO_yH_z)^+$ both in the solution [31–33] and the zeolite channels [29,34]. The copper salt hydrolysis infringes the regularities of ion exchange, incrementing the exchange level of the Cu-ZSM-5 catalysts to values above 100%. Due to the large size of these polyhydroxy copper complexes in solution, their penetration into the zeolite microchannels is minimized and the deposition of copper oxide clusters on the surface and in the zeolite mesopores is facilitated. Considering all the above assumptions, the scenarios that can be found are summarised in **Scheme 1**: scenario **a** corresponds to a 100 % exchange, where each bivalent species is associated with a Brønsted site; while scenario **b** corresponds to a 200 % exchange where each Brønsted site is occupied by a monovalent copper complex.

Therefore, considering the unit formula of a ZSM-5 with a Si/Al ratio of 25, a 200 % exchange would correspond to a Cu loading of *ca.* 3.7 wt.% [35–37]. In the case of the zeolites prepared in this work, a Cu/Al ratio value close to 0.5 would be obtained in the case of a 100 % exchange; a similar result was observed for Cu_{10}ZSM5_IE and confirmed by the calculation of the exchange percentage (%EX in **Table 1**, see *Study of the catalyst surface properties*). Cu/Al ratio exceeds the unit for the impregnated samples due to the synthesis method employed. These values are particularly affected by the abundance of precipitated copper that covers the surface and occupies the pores of the zeolite. These statements agree with the outcomes from H_2-TPR, XRD and HRTEM analysis because Cu_5ZSM5_WI and Cu_{10}ZSM5_WI contain a considerable amount of CuO. Considering Cu_{25}ZSM5_IE2, a ratio of 0.7 was observed. This could mean that multiple exchanges with a more concentrated copper solution allowed an increase in copper species (oligomeric species) per Brønsted site (**Scheme 1b**) without reaching the over-exchange of 200%. The amounts of copper present in the samples were subsequently used to estimate the H_2/Cu ratio by comparing the results obtained with the H_2-TPR technique (see *Study of the catalyst surface properties*). In this way, it was possible to estimate the type of copper species most commonly present in each catalyst.



Scheme 1: Two possible scenarios of ion-exchanged Brønsted sites.

All the diffraction patterns of the synthesized solids exhibit the characteristic peaks of MFI-type materials (**Fig. 5**) [38]. Therefore, the diffractograms of the prepared Cu-ZSM-5 samples show no appreciable differences from pure ZSM-5, except for Cu_5ZSM5_WI and Cu_{10}ZSM5_WI. More in detail, Cu_{10}ZSM5_WI distinctly shows two peaks at 2θ = 35.5° and 38.7°, while sample Cu_5ZSM5_WI is characterized only by the weak peak at 38.7°, due to the formation of bulky CuO at the external surface of the zeolite particles [39]. Contrary, the other catalysts do not present these diffraction lines, so copper could be considered to be located within the pores and channels of the parent zeolite, after it was exchanged for the proton, forming a metal complex inside the channels that cannot be detected via XRD [40,41].

Both impregnation and ion exchange influenced the value of the specific surface area (S_{BET}) of the samples compared to the parent H-ZSM-5 (423 $m^2\ g^{-1}$, 0.22 $cm^3\ g^{-1}$), with a decrease in both S_{BET} and total pore volume values (**Table 1**). In general, the greatest decreases were observed for the materials with higher copper content, i.e., Cu_{10}ZSM5_WI (329 $m^2\ g^{-1}$, 0.18 $cm^3\ g^{-1}$) among the impregnated samples, and Cu_{25}ZSM5_IE2 (359 $m^2\ g^{-1}$, 0.20 $cm^3\ g^{-1}$) among the exchanged ones. These results may suggest the presence of CuO aggregates not only outside but also inside the zeolite cavities, partially obstructing some pores.

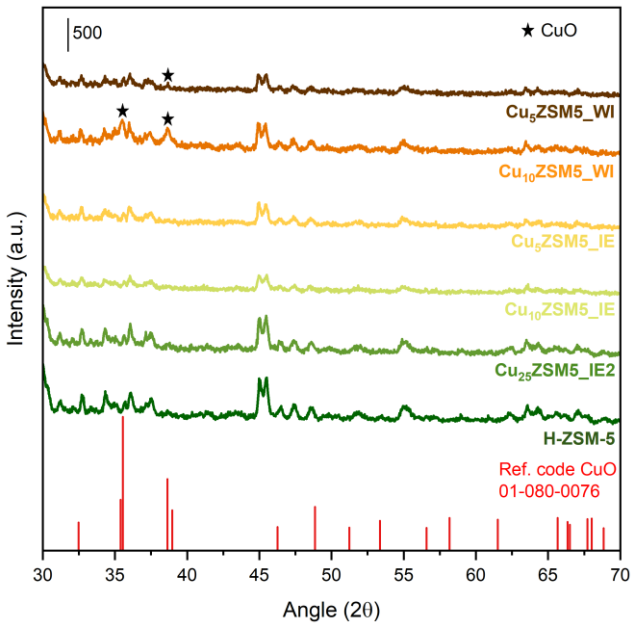


Figure 5. Diffraction patterns of the as-prepared Cu-ZSM-5 catalysts compared to the parent commercial H-ZSM-5 and the reference code of CuO.

Study of the catalyst surface properties

Cu 2p XPS spectra of all Cu-containing samples are depicted in **Fig. S2, Section a** (*Supporting Information file*). A typical CuO spectrum exhibits two strong peaks at 933.6 eV and 953.5 eV and their associated satellite peaks [42]. The samples prepared in this work show spectra with gradually decreasing intensity following the loaded copper content. Hence, Cu_{10}ZSM5_WI possesses the clearest spectrum in the series, with one peak at BE near 933 eV in the Cu $2p_{3/2}$ region and another one at nearly 953 eV in the Cu $2p_{1/2}$ region. All spectra then show a slight shift of their signals to smaller BEs attributable to the pronounced presence of Cu_2O species on the surface of the materials [42]. Considering the samples with a lower Cu loading, they are characterized by even weaker signals, suggesting a scarce presence of Cu on the zeolite surface. Therefore, due to the complexity of detecting and deconvoluting Cu^+ and Cu^0 species in the Cu 2p core level, Cu LMM Auger spectra of the samples were also analysed to have a better discernment. Typically, peaks located at one of these three possible kinetic energies (918.6, 917.7 and 916.8 eV) in the Cu LMM Auger spectrum correspond to the presence of Cu^0, Cu^{2+} and Cu^+ species, respectively [43–46]. **Fig. S2 Section b** shows the Cu LMM Auger spectra of Cu-containing catalysts. As confirmed by the Cu 2p spectrum, all the catalysts have Cu^+ as the dominant copper species, with a peak centred at

around 916 eV. Concerning sample Cu_5ZSM5_IE, the Cu LMM spectrum is particularly noisy, and a precise assignment is difficult, mainly because of the very low Cu loading.

Fig. 6 shows the H_2-TPR profiles of the as-prepared catalysts. Scientific literature has often been divided in the explanation of the reduction signals of copper species in Cu-zeolite systems; indeed, a variety of copper species that might exist in this kind of samples, including exchanged copper (II) ions (zCu^{2+}), exchanged copper (I) ions (zCu^{+}), segregated CuO particles, and Cu_xO_y structures with extra-lattice oxygen (ELO). Furthermore, the size, location (inside or outside the pores) and distribution of CuO nanoparticles might vary, thus influencing the position of the single reduction step to Cu^0, e.g., at lower temperatures with greater dispersion [16,47]. Several studies demonstrated that the reduction of Cu species in zeolites occurs in three temperature ranges: the reduction of isolated Cu^{2+} to Cu^+ and/or Cu^0 below 250 °C, the reduction of bulk CuO species on the external zeolite surface to metallic Cu^0 around 300 °C, and finally the reduction of isolated Cu^+ to Cu^0 above 300 °C [40,48,49]. According to the literature [50,51], the reduction steps of zCu^{2+} are two: $zCu^{2+} + ½\ H_2 \rightarrow zCu^+$, and $zCu^+ + ½\ H_2 \rightarrow zCu$. Consequently, the H_2-TPR profile would be characterized by two equivalent peaks at low and high temperatures, respectively, if all zCu were present as copper (II), namely in the absence of self-reduction phenomena [52–54].

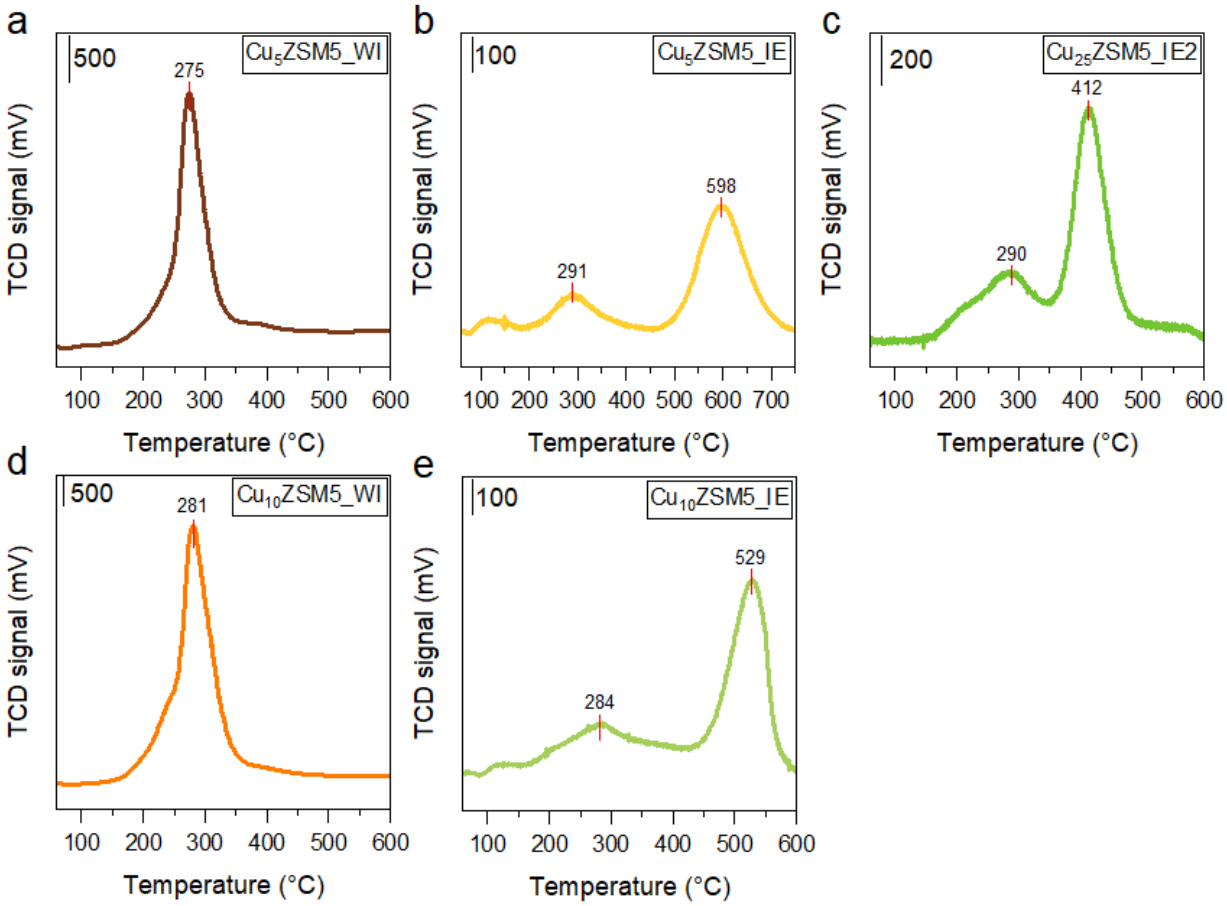


Figure 6. H_2-TPR profiles of **a)** Cu_5ZSM5_WI, **b)** Cu_5ZSM5_IE, **c)** $Cu_{25}ZSM5_IE2$, **d)** $Cu_{10}ZSM5_WI$, and **e)** $Cu_{10}ZSM5_IE$.

Contrarily, the incidence of self-reduction during He pre-treatment would result in a decrease of the first H_2 consumption, which is a condition observed for the samples prepared by ion exchange, which showed two distinct signals. The lower H_2 consumption of the first peak is consistent with the occurrence of self-reduction during the He pre-treatment. Furthermore, only with Cu_5ZSM5_IE and $Cu_{10}ZSM5_IE$, the second reduction peak is observed at temperatures higher than 450 °C (i.e., 598 and 529 °C, respectively). Actually, Bulánek et al. [40] showed that the last peak position in Cu-ZSM-5 H_2-TPR profiles is shifted to a higher temperature at decreasing copper contents. Indeed, compared to Cu_5ZSM5_IE and $Cu_{10}ZSM5_IE$, the $Cu_{25}ZSM5_IE2$ sample shows a consistent shift of the second reduction peak towards lower temperatures. Cu_5ZSM5_WI and $Cu_{10}ZSM5_WI$ samples (**Fig. 6a** and **6d**) exhibit a single asymmetric reduction peak with a maximum at 275 °C and 281 °C, respectively, with shoulders before and after the main signal. In these cases, all the copper is reduced within 400 °C. The single peak includes the reduction of both exchanged Cu species and CuO aggregates with different sizes (e.g., large particles on the outer surface and smaller clusters within channels). For these samples, the two-step reduction of exchanged species occurs in a narrow temperature range and overlaps with the reduction of bulk CuO. As a whole, TPR results suggest that the reductive capacity of Cu could be linked with catalytic behaviour: impregnated catalysts (easier reduction) exhibit higher abatement yields and very similar oscillatory behaviour. $Cu_{25}ZSM5_IE2$ also possesses a certain abatement yield and pronounced

oscillatory properties and is more easily reduced than Cu_5ZSM5_IE and Cu_{10}ZSM5_IE (which instead have higher reduction temperature and low catalytic activity).

Considering the two-steps reduction of exchanged species and the one-step reduction of CuO, the H_2-to-Cu molar ratio calculation (H_2/Cu, i.e. the ratio between the total consumption of H_2 and the total amount of Cu measured by ICP) allows to correlate the reduction profiles obtained with the copper species present in the sample. The occurrence of 100 % Cu(II) would correspond to a H_2/Cu ratio of 1.0; instead, a H_2/Cu ratio of 0.5 would indicate a totality of Cu(I) species. The quantitative results of H_2-TPR along with the H_2/Cu ratio are provided in **Table 2** and agree with the outcomes of XPS analysis. All samples mainly contain Cu(I) species, since no sample achieves an H_2/Cu ratio close to unity.

These Cu (I) species could be present either on the surface of oxide particles (or small clusters) or as exchanged ions. The highest H_2/Cu found for Cu_{10}ZSM5_WI (*i.e.*, 0.71 corresponding to 42% of Cu(II)) is likely due to the presence of bulk CuO onto the outer zeolite surface, as also evidenced by XRD (**Fig. 5**) and transmission electron microscopy. Indeed, STEM images of this sample (**Fig. 7a**) are characterised by a high number of small white spots ascribable to Cu species (EDX analysis). The average particle diameter was calculated by statistical analysis from the STEM images, which led to a value of 3.3 nm.

Regarding the other samples, lower and similar H_2/Cu values were obtained (0.64 – 0.66), suggesting the existence of comparable fractions of Cu (II) species able to undergo self-reduction. These latter likely include both exchanged zCu^{2+} species and the above-mentioned structures with ELO. The % Cu(II) calculated for all ion exchanged samples is in good agreement with the relative magnitude of the two peaks associated with the two-steps reduction mechanism. Indeed, hydrogen consumption related to the first peak roughly corresponds to 30% of the total. STEM-EDX maps of Cu_{10}ZSM5_IE confirm the absence of CuO clusters and the presence of copper in the form of exchanged species (**Fig. S3** in the *Supporting Information file*). Instead, the STEM images of the Cu_{25}ZSM5_IE2 sample (**Fig. 7b**) pointed out the presence of some CuO nanoparticles (average value of 3.0 nm) well dispersed onto the outer surface.

Table 2: Quantitative evaluations determined from the H_2-TPR and speciation through XPS analysis.

Sample	H_2 consumption ($\mu mol\ g^{-1}$) [(a)]	H_2/Cu [(a)]	% Cu (II) (atomic %) [(b)]	Predominant Cu species [(c)]
Cu_5ZSM5_WI	331	0.66	31	Cu (I)
Cu_{10}ZSM5_WI	663	0.71	42	Cu (I)
Cu_5ZSM5_IE	99	0.65	30	Cu (I)
Cu_{10}ZSM5_IE	108	0.64	27	Cu (I)
Cu_{25}ZSM5_IE2	186	0.66	33	Cu (I)

(a) H_2-TPR analysis
(b) Relative abundance of copper (II) species calculated from H_2/Cu ratio.
(c) XPS analysis

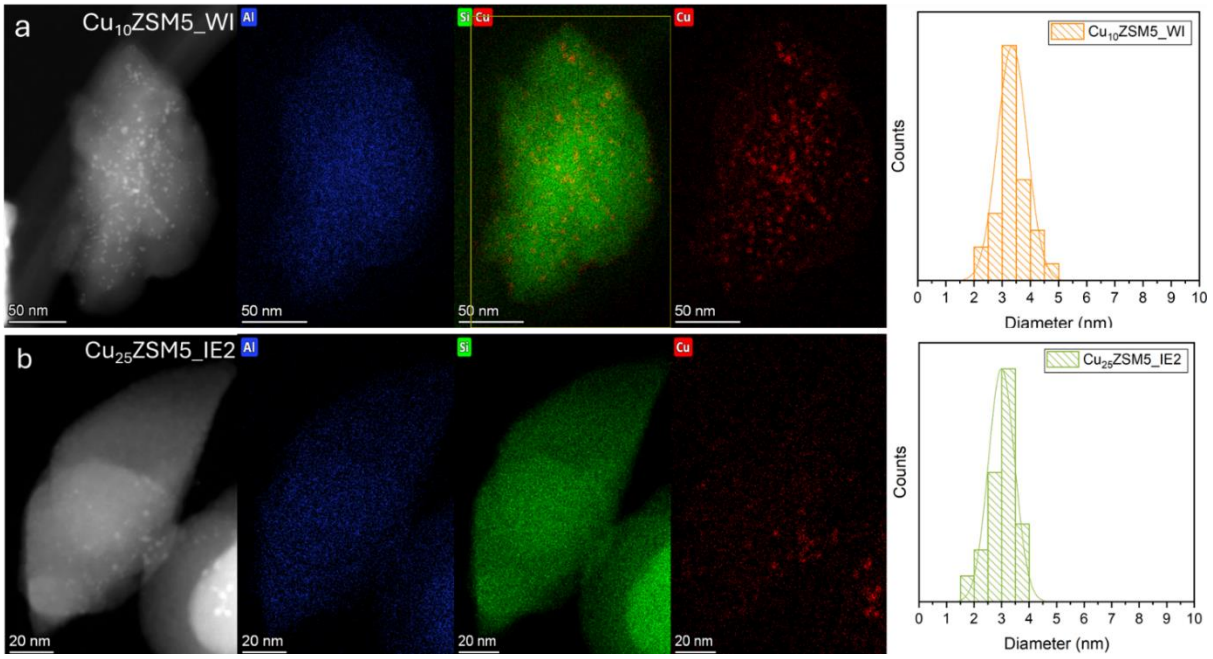


Figure 7. STEM images and associated EDX maps indicative of Al, Si and Cu distributions **(a)** of the Cu_{10}ZSM5_WI and **(b)** Cu_{25}ZSM5_IE2 samples; size distributions of copper particles are reported alongside the EDX maps.

FT-IR measurements were carried out on the pristine H-ZSM-5 zeolite and on the as-prepared Cu-ZSM-5 samples to study the consumption of Brønsted acidic sites after synthesis procedures. The spectra were collected after a vacuum activation at 500 °C for 1 h. A magnification of the hydroxyl stretching region is depicted in **Fig. 8**. All the spectra are marked by different components present in the 3800-3400 cm^{-1} spectral range. Typically, the well-defined sharp band at 3745 cm^{-1} is ascribed to virtually isolated Si-OH groups located on the external surface of the zeolite [55–57]; the weak shoulder between 3740-3700 cm^{-1} is generated by weakly perturbed Si-OH species. These latter are principally positioned inside the zeolite framework in final position and can form hydrogen-bonded silanols chains due to the presence of defects, such as nanovoids by silicon vacancies. At 3670 cm^{-1}, a band ascribable to extra-framework Al-OH species can be recognised in all samples [58]. The band indicating the presence of strongly acidic bridging Si-(OH)-Al Brønsted sites is sited at around 3610 cm^{-1} [59–61]. Finally, an unresolved broad band centred at around 3500 cm^{-1} is particularly evident for the Cu_5ZSM5_WI, Cu_{10}ZSM5_WI, and Cu_{10}ZSM5_IE catalysts. This feature signals the presence of internal cavities (defects) with adjacent OH groups mutually interacting via medium-strength hydrogen bonds.

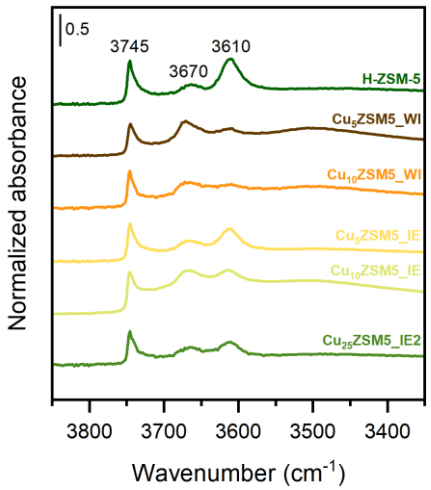


Figure 8. FT-IR spectra of the H-ZSM-5 and the Cu-ZSM-5 samples in the hydroxyl stretching region.

By the intensity ratio between the integrated IR absorbance of the 3610 cm^{-1} band in the pristine zeolite and of the same band in the other materials it is possible to estimate the degree of ion exchange that occurred for the exchanged and impregnated samples (%EX) listed in **Table 1**. Impregnated samples achieved a higher and almost identical degree of exchange, while ion-exchanged samples showed the lowest %EX values, namely 33% (Cu_5ZSM5_IE) and 58 %EX (Cu_{10}ZSM5_IE). Markedly, the double ion-exchange with a more concentrated Cu solution led to higher Cu content but did not yield an increase in % EX. (*i.e.*, 54% for Cu_{25}ZSM5_IE2). Two possible reasons could explain such discrepancy, namely *i)* the presence of exchanged species containing more than one Cu atom (as oligomeric species $[Cu_xO_yH_z]^+$ reported in Scheme 1b); *ii)* the presence of CuO, dispersed onto the external zeolite surface. As the latter is concerned, XRD (**Fig. 5**) does not give evidence of bulk CuO particles on Cu_{25}ZSM5_IE2, and STEM images (**Fig. 7b**) showed only scarce amount of CuO nanoparticles. Moreover, H_2-TPR of Cu_{25}ZSM5_IE2 seems to exclude a relevant amount of CuO particles, showing a profile similar to that of other ion-exchanged samples (without an evident sharp peak at ca. 280°C). On the other hand, the consistent shift of the second reduction peak towards lower temperature observed for this sample could be due to the easier reducibility of oligomeric species with respect to isolated exchanged copper species.

In order to gain an in-depth understanding of the reasons for the oscillating behaviour of some selected samples, *in situ* FT-IR spectroscopic studies were conducted. The operating protocol involves the interaction of N_2O with Cu-zeolites to observe the possible formation of nitrate species, as fully described in the *Materials and experimental methods* section above. This type of experiment was performed to demonstrate whether nitrate formation is linked to the oscillatory catalytic activity of Cu-ZSM-5 catalysts, as already witnessed in kinetic and transient experiments reported in the literature [62,63,20]. In particular, Ochs and Turek proposed a mechanism that would describe the oscillatory behaviour through six phases:

$$N_2O + 2\text{⁘} \rightarrow O_s + N_2 \quad \text{(a)}$$

$$2O_s \rightarrow O_2 + 4\text{⁘} \quad \text{(b)}$$

$$N_2O + O_s \rightarrow 2NO + 2\text{⁘} \quad \text{(c)}$$

$$NO + 2O_s \rightarrow NO_{3,s} + 3\text{⁘} \quad \text{(d)}$$

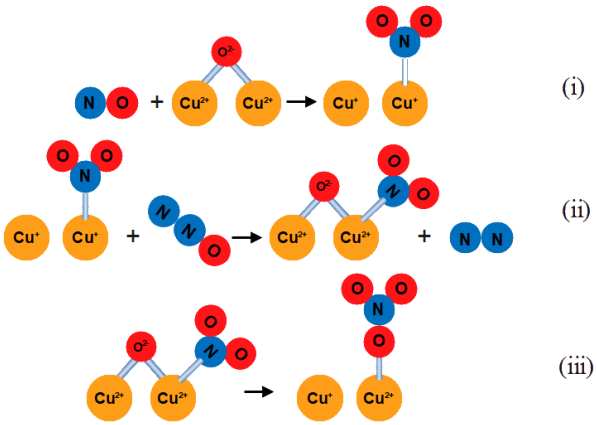
$$NO_{3,s} \rightarrow NO + O_2 + \text{⁘} \quad \text{(e)}$$

$$N_2O + O_s \rightarrow O_2 + N_2 + 2\text{⁘} \quad \text{(f)}$$

where ⁘ denotes an active site (two adjacent Cu^+), O_s atomic oxygen species, and $NO_{3,s}$ nitrate intermediate [20]. In the first reaction (a) N_2 and atomic oxygen are formed by nitrous oxide decomposition, without the adsorption of N_2O on the catalyst. This step requires two sufficiently nearby active sites, namely two Cu^+ ions, to facilitate the formation of oxygen bridges (Cu^{2+}–O–Cu^{2+}) useful for reaction propagation. Then, a decrease of the N_2O decomposition activity is due to a rapid development of a high oxygen coverage, due to the low rate of the recombination of atomic oxygen

in (b). After the formation of gaseous NO at the reaction site in (c), this reacts with atomic oxygen species to give NO_3 according to step (d) with a high reaction rate (no NO adsorption band visible in the 1900-1800 cm^{-1} region of IR spectra, **Fig. 9**). Adsorbed nitric oxide and nitrogen dioxide must exist as intermediates, thus the reaction (c) and (d) are simplifications. Oxidized copper sites are required to convert NO to NO_2 and, $NO_{3,s}$ should be stable as long as enough O_s is available. Investigating Ochs and Turek's model, Fanson et al. [22] identified some unclear points of the mechanism, such as the need for a pair of Cu ions very close together with an absorbed oxygen for progressive oxidation of the nitric oxide formed in step (c).

They proposed an alternative pathway (**Scheme 2**) for step (c), where the previously formed NO reacts with a bridged oxygen atom giving adsorbed NO_2, reducing one pair of Cu ions (i). The renewed active site (2 Cu^+) is able to react with an additional N_2O molecule to establish a new oxygen bridge (ii). Finally, an adsorbed monodentate nitrate species $NO_{3,s}$ can be produced due to the combination of adsorbed NO_2 and the bridged oxygen (iii). This combination can also occur between a desorbed NO_2 and an oxygen in a non-neighbouring location [22].



Scheme 2. Schematization of the proposed reaction mechanism operating for the formation of nitrate species on the surface of Cu-ZSM-5. Figure adapted from Fanson et al. [22].

The outcomes of variable temperature experiments on three catalysts taken as a model are depicted in **Fig. 9** (complete spectra are reported in **Fig. S4** in the *Supporting Information file*). All three catalysts exhibit the characteristic signals of the interaction between the copper sites and N_2O probe molecule after exposure of the samples to approximately 30 mbar of gas. The small IR adsorption peak at 2291 cm^{-1} with a pronounced shoulder at 2275 cm^{-1} can be assigned to the N–N stretch of N_2O bound to a Cu^+ site; on the other hand, the signal at 2219 cm^{-1} is assigned to N_2O weakly bound to the zeolite framework [23]. The formation of nitrate species is particularly noticeable for samples Cu_{10}ZSM5_WI and Cu_{25}ZSM5_IE2, which exhibit oscillating behaviour in the test session. The corresponding peak at 1624 cm^{-1}, which can be ascribed to the anti-symmetric stretching of monodentate nitrate bound to a copper site [23], appears at different times in the stationary phase of the analysis: as soon as 400 °C is reached for Cu_{25}ZSM5_IE2 (**Fig. 9c**) and after 30 min for Cu_{10}ZSM5_WI (Section A). No appreciable peak was observed for Cu_{10}ZSM5_IE (**Fig. 9b**).

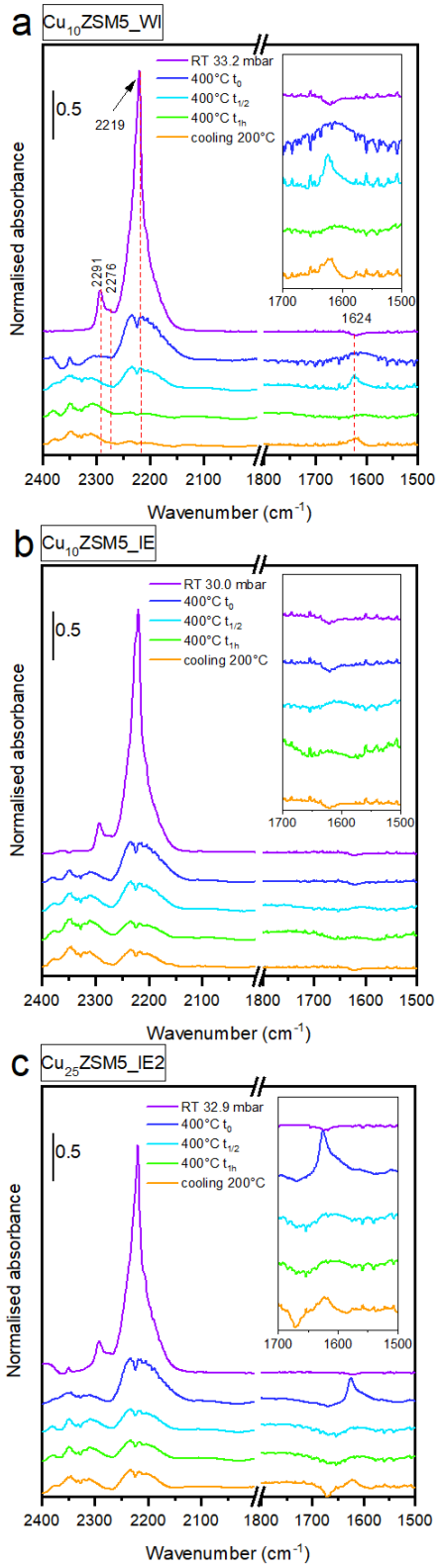


Figure 9. FT-IR spectra collected during variable temperature experiments with N_2O gas for **(a)** Cu_{10}ZSM5_WI, **(b)** Cu_{10}ZSM5_IE, and **(c)** Cu_{25}ZSM5_IE2

These findings confirm the mechanism of nitrate formation reported above and may offer some explanation for the different induction times and oscillation frequencies between the two samples. Cu_{25}ZSM5_IE2 showed an induction time of 20 min during the test at 400 °C while, on the other hand, about 30 min were required before oscillations were observed for the two impregnated samples.

Conclusions

In this work, a set of Cu-ZSM-5 catalysts was prepared through wet impregnation (WI) and ion-exchange methods (IE). Their physical-chemical characteristics were analysed via complementary techniques and catalytic decomposition tests were performed with 1000 ppm N_2O. As a whole, only three catalysts exhibited effective catalytic activities, namely Cu_5ZSM5_WI (average of 66 % of conversion), Cu_{10}ZSM5_WI (average of 72 % of conversion), and Cu_{25}ZSM5_IE2 (average of 26 % of conversion). Cu_5ZSM5_WI and Cu_{10}ZSM5_WI possessed comparable yields and oscillating profiles (in terms of N_2O conversion), while Cu_{25}ZSM5_IE2 achieved lower yields and greater shape and intensity oscillations. In contrast, Cu_5ZSM5_IE and Cu_{10}ZSM5_IE exhibited minor catalytic activity. The characterisation results revealed some correlations between catalytic behaviours and physico-chemical properties. Specifically, it was observed that the samples with higher reductive capacities also demonstrated oscillating catalytic behaviour. FT-IR analysis on the Brønsted sites revealed that good levels of ion exchange were obtained through the wet impregnation technique. Cu_{25}ZSM5_IE2, despite having an exchange level of ca. 58 %, still had a higher amount of Cu. These copper species could be present as oligomeric complexes (Cu/Al ratio = 0.7), as attested by H_2-TPR analysis and FT-IR. In addition, the outcomes of variable temperature experiments on three catalysts confirmed the formation of nitrate species for samples Cu_{10}ZSM5_WI, and Cu_{25}ZSM5_IE2. Reproducibility tests confirmed that under specific conditions, the decomposition of N_2O over Cu-ZSM-5 catalysts can give rise to self-organized patterns or uniform oscillations. The same catalyst showed a higher oscillation frequency if the test was performed with a lower spatial velocity. This result could confirm that spatial velocity influences the deposition-coverage phenomena of active copper sites. Finally, under different operational conditions, the same catalyst can exhibit chaotic behaviour (in terms of N_2O conversion). This type of behaviour is characterized by a complex and unpredictable response from the system. Although it is deterministic at a fundamental level, it appears random and lacks a clear pattern over time. Such chaos in catalytic reactions indicates a highly sensitive dependence on initial conditions, where slight variations can lead to significantly divergent outcomes, contrasting with the orderly and repetitive nature of Oscillatory Turing Patterns. This duality in behaviour underscores the sensitivity of Cu-ZSM-5 catalysed reactions to operational conditions and highlights the intricate balance between order and chaos in chemical reaction systems. Understanding these dynamics is crucial for optimizing catalytic processes and designing reactors that can harness the benefits of both ordered patterns and chaotic dynamics for improved efficiency and selectivity in chemical production.

Declaration of Competing Interest

The authors declare that they have no known competing financial interests or personal relationships that could have appeared to influence the work reported in this paper.

Acknowledgements

The authors greatly thank Angelica Fusiello for helping in data collection during her MS thesis preparation. Camilla Galletti, Marco Allione and Salvatore Guastella are kindly acknowledged as well for performing XRD, TEM and XPS analyses. The authors acknowledge the funding received by the Italian Ministero dell'Università e della Ricerca (MUR) under the Dipartimento di Eccellenza 2018–2022 program and the PON Ricerca e Innovazione "REACT-EU" project (DM 1062/21).

Keywords: N_2O decomposition, Cu-ZSM-5, isothermal oscillations, Oscillatory Turing Patterns

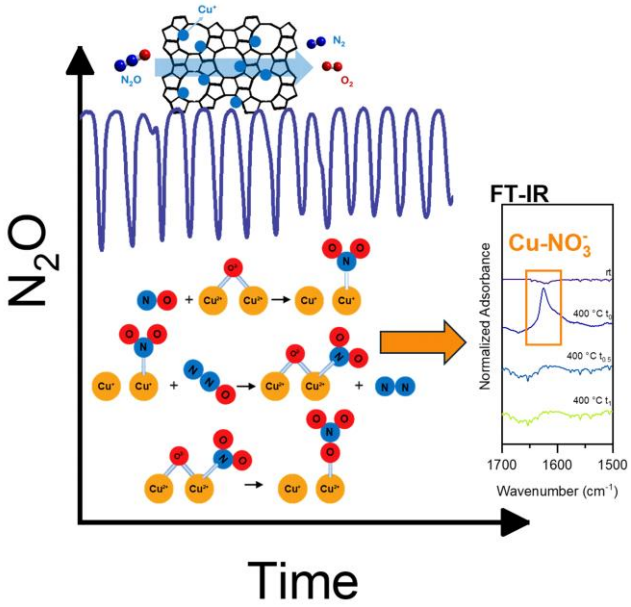
References

1. Chen, H.-Y. (2014) Cu/Zeolite SCR Catalysts for Automotive Diesel NOx Emission Control, in *Urea-SCR Technology for deNOx After Treatment of Diesel Exhausts* (eds.Nova, I., and Tronconi, E.), Springer New York, New York, NY, pp. 123–147.
2. Sjövall, H., Olsson, L., Fridell, E., and Blint, R.J. (2006) Selective catalytic reduction of NOx with NH3 over Cu-ZSM-5—The effect of changing the gas composition. *Applied Catalysis B: Environmental*, **64** (3–4), 180–188.
3. Piumetti, M., Bensaid, S., Fino, D., and Russo, N. (2015) Catalysis in Diesel engine NO_x aftertreatment: a review. *Catalysis, Structure & Reactivity*, **1** (4), 155–173.
4. Frutos, O.D., Quijano, G., Aizpuru, A., and Muñoz, R. (2018) A state-of-the-art review on nitrous oxide control from waste treatment and industrial sources. *Biotechnology Advances*, **36** (4), 1025–1037.
5. Tian, H., Xu, R., Canadell, J.G., Thompson, R.L., Winiwarter, W., Suntharalingam, P., Davidson, E.A., Ciais, P., Jackson, R.B., Janssens-Maenhout, G., Prather, M.J., Regnier, P., Pan, N., Pan, S., Peters, G.P., Shi, H., Tubiello, F.N., Zaehle, S., Zhou, F., Arneth, A., Battaglia, G., Berthet, S., Bopp, L., Bouwman, A.F., Buitenhuis, E.T., Chang, J., Chipperfield, M.P., Dangal, S.R.S., Dlugokencky, E., Elkins, J.W., Eyre, B.D., Fu, B., Hall, B., Ito, A., Joos, F., Krummel, P.B., Landolfi, A., Laruelle, G.G., Lauerwald, R., Li, W., Lienert, S., Maavara, T., MacLeod, M., Millet, D.B., Olin, S., Patra, P.K., Prinn, R.G., Raymond, P.A., Ruiz, D.J., Van Der Werf, G.R., Vuichard, N., Wang, J., Weiss, R.F., Wells, K.C., Wilson, C., Yang, J., and Yao, Y. (2020) A comprehensive quantification of global nitrous oxide sources and sinks. *Nature*, **586** (7828), 248–256.

6. Salomone, F., Bonura, G., Frusteri, F., Castellino, M., Fontana, M., Chiodoni, A.M., Russo, N., Pirone, R., and Bensaid, S. (2022) Physico-Chemical Modifications Affecting the Activity and Stability of Cu-Based Hybrid Catalysts during the Direct Hydrogenation of Carbon Dioxide into Dimethyl-Ether. *Materials*, **15** (21), 7774.
7. Salomone, F., Sartoretti, E., Ballauri, S., Castellino, M., Novara, C., Giorgis, F., Pirone, R., and Bensaid, S. (2023) CO2 hydrogenation to methanol over Zr- and Ce-doped indium oxide. *Catalysis Today*, **423**, 114023.
8. Ballauri, S., Sartoretti, E., Hu, M., D'Agostino, C., Ge, Z., Wu, L., Novara, C., Giorgis, F., Piumetti, M., Fino, D., Russo, N., and Bensaid, S. (2023) Praseodymium doping in ceria-supported palladium nanocatalysts as an effective strategy to minimize the inhibiting effects of water during methane oxidation. *Applied Catalysis B: Environmental*, **320**, 121898.
9. Rizzetto, A., Piumetti, M., Pirone, R., Sartoretti, E., and Bensaid, S. (2024) Study of ceria-composite materials for high-temperature CO2 capture and their ruthenium functionalization for methane production. *Catalysis Today*, **429**, 114478.
10. Mezzapesa, M.P., Salomone, F., Guzmán, H., Zammillo, F., Millini, R., Bua, L., Marra, G., Tacca, A., Marrazzo, R., Russo, N., Pirone, R., Hernandez, S., and Bensaid, S. (2024) Development of In-Cu binary oxides catalysts for hydrogenating CO2 via thermocatalytic and electrocatalytic routes. *Inorg. Chem. Front.*, 10.1039.D3QI02499G.
11. Lintz, H.-G., and Turek, T. (1995) Isothermal oscillations in the catalytic decomposition of nitrous oxide over Cu-ZSM-5. *Catal Lett*, **30** (1–4), 313–318.
12. Ciambelli, P., Garufi, E., Pirone, R., Russo, G., and Santagata, F. (1996) Oscillatory behaviour in nitrous oxide decomposition on over-exchanged Cu-ZSM-5 zeolite. *Applied Catalysis B: Environmental*, **8** (3), 333–341.
13. Slin'ko, M.G., and Slin'ko, M.M. (1980) Auto-oscillations in the Rates of Heterogeneous Catalytic Reactions. *Russ. Chem. Rev.*, **49** (4), 295–309.
14. Elnashaie, S., and Elshishini, S.S. (1996) *Dynamic modelling, bifurcation and chaotic behaviour of gas-solid catalytic reactors*, Gordon & Breach, South Yarra, Victoria].
15. Ciambelli, P., Di Benedetto, A., Garufi, E., Pirone, R., and Russo, G. (1998) Spontaneous Isothermal Oscillations in N2O Decomposition over a Cu–ZSM5 Catalyst. *Journal of Catalysis*, **175** (2), 161–169.
16. Armandi, M., Andana, T., Bensaid, S., Piumetti, M., Bonelli, B., and Pirone, R. (2020) Effect of the preparation technique of Cu-ZSM-5 catalysts on the isothermal oscillatory behavior of nitrous oxide decomposition. *Catalysis Today*, **345**, 59–70.
17. Gruenert, W., Hayes, N.W., Joyner, R.W., Shpiro, E.S., Siddiqui, M.R.H., and Baeva, G.N. (1994) Structure, Chemistry, and Activity of Cu-ZSM-5 Catalysts for the Selective Reduction of NOx in the Presence of Oxygen. *J. Phys. Chem.*, **98** (42), 10832–10846.
18. Pirone, R., Garufi, E., Ciambelli, P., Moretti, G., and Russo, G. (1997) Transient behaviour of Cu-overexchanged ZSM-5 catalyst in NO decomposition. *Catalysis Letters*, **43** (3/4), 255–259.
19. Shpiro, E.S., Grünert, W., Joyner, R.W., and Baeva, G.N. (1994) Nature, distribution and reactivity of copper species in over-exchanged Cu-ZSM-5 catalysts: an XPS/XAES study. *Catal Lett*, **24** (1–2), 159–169.
20. Ochs, T., and Turek, T. (1999) The mechanism of kinetic oscillations in the catalytic N2O decomposition over Cu-ZSM-5. *Chemical Engineering Science*, **54** (20), 4513–4520.
21. Liu, F., Li, Y., and Sun, X. (2013) The isothermal oscillations and fluctuation-driven oscillations of N2O decomposition over Cu-ZSM-5 zeolites. *Chemical Physics Letters*, **584**, 195–199.
22. Fanson, P.T., Stradt, M.W., Delgass, W.N., and Lauterbach, J. (2001) Infrared Evidence for the Existence of Nitrate Species on Cu-ZSM5 During Isothermal Rate Oscillations in the Decomposition of N2O. *Catal. Letters*, **77** (1–3), 15–19.
23. Shelef, M. (1995) Selective Catalytic Reduction of NOx with N-Free Reductants. *Chem. Rev.*, **95** (1), 209–225.
24. Pirone, R. (1996) Nitric oxide decomposition over Cu-exchanged ZSM-5 with high Si/Al ratio. *Applied Catalysis B: Environmental*, **8** (2), 197–207.
25. Piumetti, M. (2022) *Molecular Dynamics and Complexity in Catalysis and Biocatalysis*, Springer International Publishing, Cham.
26. Turing, A.M. (1952) The chemical basis of morphogenesis. *Phil. Trans. R. Soc. Lond. B*, **237** (641), 37–72.
27. Arévalo-Hidalgo, A.G., Santana, J.A., Fu, R., Ishikawa, Y., and Hernández-Maldonado, A.J. (2010) Separation of CO2 from light gas mixtures using nanoporous silicoaluminophosphate sorbents: Effect of multiple-step ion exchange and adsorption mechanism via computational studies. *Microporous and Mesoporous Materials*, **130** (1–3), 142–153.
28. Yashnik, S.A., Ismagilov, Z.R., and Anufrienko, V.F. (2005) Catalytic properties and electronic structure of copper ions in Cu-ZSM-5. *Catalysis Today*, **110** (3–4), 310–322.
29. Iwamoto, M., Yahiro, H., Tanda, K., Mizuno, N., Mine, Y., and Kagawat, S. (1991) Removal of Nitrogen Monoxide through a Novel Catalytic Process. 1. Decomposition on Excessively Copper Ion Exchanged ZSM-5 Zeolites. *J. Phys. Chem.*, **95**, 3727–3730.
30. Valyon, J., and Keith Hall, W. (1993) On the preparation and properties of CuZSM-5 catalysts for NO decomposition. *Catal Lett*, **19** (2–3), 109–119.
31. Yahiro, H., and Iwamoto, M. (2001) Copper ion-exchanged zeolite catalysts in deNOx reaction. *Applied Catalysis A: General*, **222** (1–2), 163–181.
32. Yashnik, S.A., Salnikov, A.V., Vasenin, N.T., Anufrienko, V.F., and Ismagilov, Z.R. (2012) Regulation of the copper-oxide cluster structure and DeNOx activity of Cu-ZSM-5 catalysts by variation of OH/Cu2+. *Catalysis Today*, **197** (1), 214–227.
33. Yashnik, S.A., Surovtsova, T.A., and Salnikov, A.V. (2024) Cu-ZSM-5 catalyst synthesis via ion-exchange with ammonia solution of copper hydroxysalts. *Microporous and Mesoporous Materials*, **367**, 112966.
34. Smeets, P., Groothaert, M., Vanteeffelen, R., Leeman, H., Hensen, E., and Schoonheydt, R. (2007) Direct NO and N2O decomposition and NO-assisted N2O decomposition over Cu-zeolites: Elucidating the influence of the CuCu distance on oxygen migration. *Journal of Catalysis*, **245** (2), 358–368.
35. Dedecek, J., Sobalik, Z., Tvaruazkova, Z., Kaucky, D., and Wichterlova, B. (1995) Coordination of Cu Ions in High-Silica Zeolite Matrixes. Cu+ Photoluminescence, IR of NO Adsorbed on Cu2+, and Cu2+ ESR Study. *J. Phys. Chem.*, **99** (44), 16327–16337.
36. Gao, F., Washton, N.M., Wang, Y., Kollár, M., Szanyi, J., and Peden, C.H.F. (2015) Effects of Si/Al ratio on Cu/SSZ-13 NH3-SCR catalysts: Implications for the active Cu species and the roles of Brønsted acidity. *Journal of Catalysis*, **331**, 25–38.
37. Jabłońska, M., Góra-Marek, K., Bruzzese, P.C., Palčić, A., Pyra, K., Tarach, K., Bertmer, M., Poppitz, D., Pöppl, A., and Gläser, R. (2022) Influence of Framework n(Si)/ n(Al) Ratio on the Nature of Cu Species in Cu-ZSM-5 for NH3 -SCR-DeNOx. *ChemCatChem*, **14** (18), e202200627.
38. Kokotailo, G.T., Lawton, S.L., Olson, D.H., and Meier, W.M. (1978) Structure of synthetic zeolite ZSM-5. *Nature*, **272** (5652), 437–438.
39. Dosa, M., Marin-Figueredo, M.J., Sartoretti, E., Novara, C., Giorgis, F., Bensaid, S., Fino, D., Russo, N., and Piumetti, M. (2022) Cerium-Copper Oxides Synthesized in a Multi-Inlet Vortex Reactor as Effective Nanocatalysts for CO and Ethene Oxidation Reactions. *Catalysts*, **12** (4), 364.

40. Bulánek, R., Wichterlová, B., Sobalık, Z., and Tichý, J. (2001) Reducibility and oxidation activity of Cu ions in zeolites Effect of Cu ion coordination and zeolite framework composition.
41. Santa Cruz-Navarro, D., Torres-Rodríguez, M., Gutiérrez-Arzaluz, M., Mugica-Álvarez, V., and Pergher, S.B. (2022) Comparative Study of Cu/ZSM-5 Catalysts Synthesized by Two Ion-Exchange Methods. *Crystals*, **12** (4), 545.
42. Biesinger, M.C. (2017) Advanced analysis of copper X-ray photoelectron spectra. *Surface & Interface Analysis*, **49** (13), 1325–1334.
43. Saikova, S., Vorobyev, S., Likhatski, M., Romanchenko, A., Erenburg, S., Trubina, S., and Mikhlin, Y. (2012) X-ray photoelectron, Cu L3MM Auger and X-ray absorption spectroscopic studies of Cu nanoparticles produced in aqueous solutions: The effect of sample preparation techniques. *Applied Surface Science*, **258** (20), 8214–8221.
44. Andana, T., Piumetti, M., Bensaid, S., Veyre, L., Thieuleux, C., Russo, N., Fino, D., Quadrelli, E.A., and Pirone, R. (2017) CuO nanoparticles supported by ceria for NO x -assisted soot oxidation: insight into catalytic activity and sintering. *Applied Catalysis B: Environmental*, **216**, 41–58.
45. Sartoretti, E., Novara, C., Paganini, M.C., Chiesa, M., Castellino, M., Giorgis, F., Piumetti, M., Bensaid, S., Fino, D., and Russo, N. (2023) Investigation of Cu-doped ceria through a combined spectroscopic approach: Involvement of different catalytic sites in CO oxidation. *Catalysis Today*, **420**, 114037.
46. Cocuzza, C., Sartoretti, E., Novara, C., Giorgis, F., Bensaid, S., Russo, N., Fino, D., and Piumetti, M. (2023) Copper-manganese oxide catalysts prepared by solution combustion synthesis for total oxidation of VOCs. *Catalysis Today*, **423**, 114292.
47. Liu, Z., Amiridis, M.D., and Chen, Y. (2005) Characterization of CuO Supported on Tetragonal ZrO $_2$ Catalysts for N $_2$ O Decomposition to N $_2$. *J. Phys. Chem. B*, **109** (3), 1251–1255.
48. Sarkany, J., d'Itri, J.L., and Sachtler, W.M.H. (1992) Redox chemistry in excessively ion-exchanged Cu/Na-ZSM-5. *Catal Lett*, **16** (3), 241–249.
49. Nanba, T., Masukawa, S., Ogata, A., Uchisawa, J., and Obuchi, A. (2005) Active sites of Cu-ZSM-5 for the decomposition of acrylonitrile. *Applied Catalysis B: Environmental*, **61** (3–4), 288–296.
50. Richter, M., Fait, M.J.G., Eckelt, R., Schreier, E., Schneider, M., Pohl, M.-M., and Fricke, R. (2007) Oxidative gas phase carbonylation of methanol to dimethyl carbonate over chloride-free Cu-impregnated zeolite Y catalysts at elevated pressure. *Applied Catalysis B: Environmental*, **73** (3–4), 269–281.
51. Torre-Abreu, C., Ribeiro, M.F., Henriques, C., and Delahayb, G. (1997) NO TPD and H2-TPR studies for characterisation of CuMOR catalysts The role of Si/Al ratio, copper content and location. *plied Catalysis B: Environmental*, **14**, 261–272.
52. Turnes Palomino, G., Fisicaro, P., Bordiga, S., Zecchina, A., Giamello, E., and Lamberti, C. (2000) Oxidation States of Copper Ions in ZSM-5 Zeolites. A Multitechnique Investigation. *J. Phys. Chem. B*, **104** (17), 4064–4073.
53. Llabrés I Xamena, F.X., Fisicaro, P., Berlier, G., Zecchina, A., Palomino, G.T., Prestipino, C., Bordiga, S., Giamello, E., and Lamberti, C. (2003) Thermal Reduction of Cu^{2+} –Mordenite and Re-oxidation upon Interaction with H_2O, O_2 , and NO. *J. Phys. Chem. B*, **107** (29), 7036–7044.
54. Borfecchia, E., Lomachenko, K.A., Giordanino, F., Falsig, H., Beato, P., Soldatov, A.V., Bordiga, S., and Lamberti, C. (2015) Revisiting the nature of Cu sites in the activated Cu-SSZ-13 catalyst for SCR reaction. *Chem. Sci.*, **6** (1), 548–563.
55. Piumetti, M., Bonelli, B., Massiani, P., Millot, Y., Dzwigaj, S., Gaberova, L., Armandi, M., and Garrone, E. (2011) Novel vanadium-containing mesocellular foams (V-MCF) obtained by direct synthesis. *Microporous and Mesoporous Materials*, **142** (1), 45–54.
56. Piumetti, M., Bonelli, B., Massiani, P., Dzwigaj, S., Rossetti, I., Casale, S., Gaberova, L., Armandi, M., and Garrone, E. (2011) Effect of vanadium dispersion and support properties on the catalytic activity of V-SBA-15 and V-MCF mesoporous materials prepared by direct synthesis. *Catalysis Today*, **176** (1), 458–464.
57. Piumetti, M., Armandi, M., Garrone, E., and Bonelli, B. (2012) An IR spectroscopy assessment of the surface acidity of mesoporous VO – SiO2 catalysts. *Microporous and Mesoporous Materials*, **164**, 111–119.
58. Grahn, M., Faisal, A., Öhrman, O.G.W., Zhou, M., Signorile, M., Crocellà, V., Nabavi, M.S., and Hedlund, J. (2020) Small ZSM-5 crystals with low defect density as an effective catalyst for conversion of methanol to hydrocarbons. *Catalysis Today*, **345**, 136–146.
59. Bordiga, S., Lamberti, C., Bonino, F., Travert, A., and Thibault-Starzyk, F. (2015) Probing zeolites by vibrational spectroscopies. *Chem. Soc. Rev.*, **44** (20), 7262–7341.
60. Deplano, G., Signorile, M., Crocellà, V., Porcaro, N.G., Atzori, C., Solemsli, B.G., Svelle, S., and Bordiga, S. (2022) Titration of Cu(I) Sites in Cu-ZSM-5 by Volumetric CO Adsorption. *ACS Appl. Mater. Interfaces*, **14** (18), 21059–21068.
61. Zachariou, A., Hawkins, A.P., Howe, R.F., Skakle, J.M.S., Barrow, N., Collier, P., Nye, D.W., Smith, R.I., Stenning, G.B.G., Parker, S.F., and Lennon, D. (2023) Counting the Acid Sites in a Commercial ZSM-5 Zeolite Catalyst. *ACS Phys. Chem Au*, **3** (1), 74–83.
62. Turek, T. (1996) Kinetics of nitrous oxide decomposition over Cu-ZSM-5. *Applied Catalysis B: Environmental*, **9**, 201–210.
63. Turek, T. (1998) A Transient Kinetic Study of the Oscillating N2O Decomposition over Cu--ZSM-5. *Journal of Catalysis*, **174** (1), 98–108.

Entry for the Table of Contents



A particular feature of copper-exchanged zeolite ZSM-5 (Cu-ZSM-5) is the presence of spontaneous isothermal oscillations which take place during N_2O decomposition reaction, depending on the operating conditions. Physico-chemical investigations disclose that this behaviour could be related to the presence of more abundant and easily reducible copper species (ICP, EDX and H_2-TPR) which interacts better with the zeolitic support (FT-IR). Catalytic tests under a long time on stream suggest that either self-organised patterns or deterministic chaos can be achieved during the reaction, depending on the operating conditions, such as temperature and contact time.